

## **Revealing the switching mechanisms of an OFF-ON-OFF fluorescent logic gate system**

Weijie Chi,<sup>a</sup> Jie Chen,<sup>b</sup> Qinglong Qiao,<sup>b</sup> Ying Gao,<sup>a,c</sup> Zhaochao Xu,<sup>b</sup>  
and Xiaogang Liu<sup>a\*</sup>

<sup>a</sup>Science and Math Cluster, Singapore University of Technology and Design, 8  
Somapah Road, Singapore 487372, Singapore

<sup>b</sup>CAS Key Laboratory of Separation Science for Analytical Chemistry Dalian  
Institute of Chemical Physics, Chinese Academy of Sciences 457 Zhongshan  
Road, Dalian 116023, China.

<sup>c</sup>Jilin Engineering Normal University, Changchun, 130052, China

\* E-mail: xiaogang\_liu@sutd.edu.sg

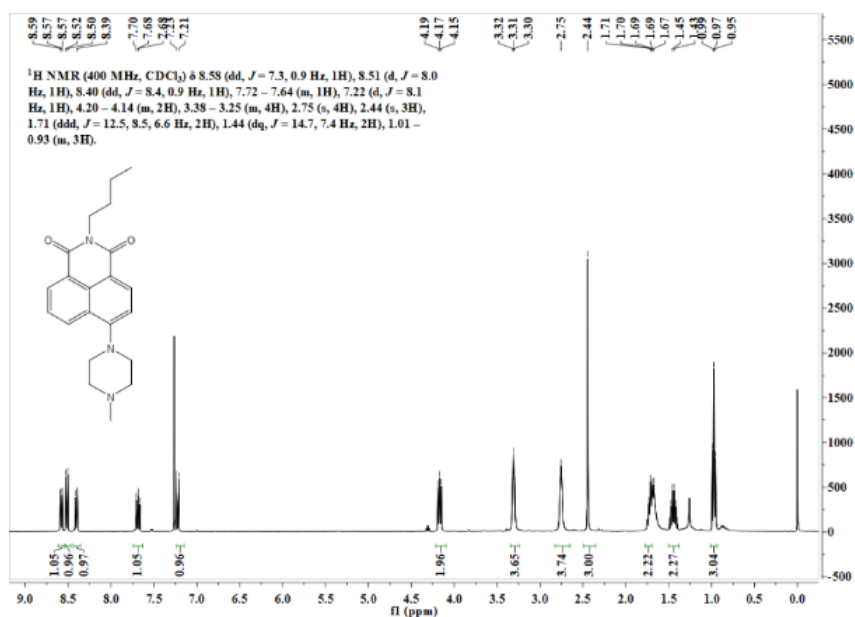


Figure S1. <sup>1</sup>H-NMR spectrum of **M3**.

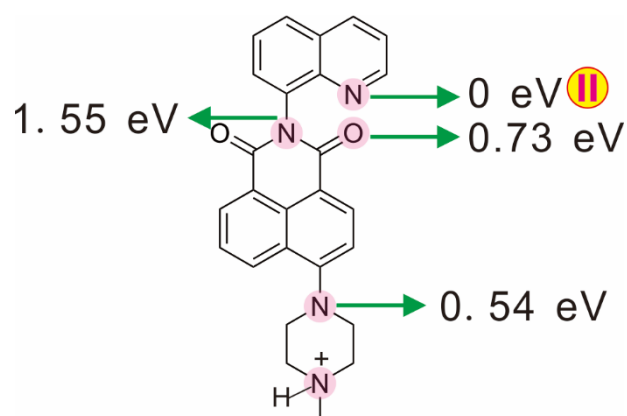


Figure S2. Possible four protonated positions of **M1-1H** and relative Gibbs free energy of the corresponding protonated products (with two protons). Site **II** shows the highest reactive activation towards protonation (forming **M1-2H**).

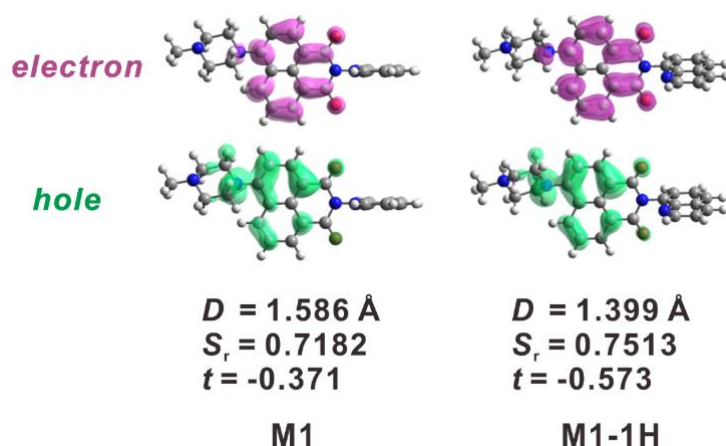


Figure S3. Distribution of hole and electron in **M1** and **M1-1H**. Green donates hole and pink for electron;  $D$  is the centroid distance of hole and electron;  $S_r$  is overlap between hole and electron;  $t$  index is designed to measure the degree of hole and electron separation in the charge transfer direction. If  $t < 0$ , hole and electron is not complete separated, and a more negative value of  $t$  indicates a smaller degree of charge transfer.<sup>1</sup>

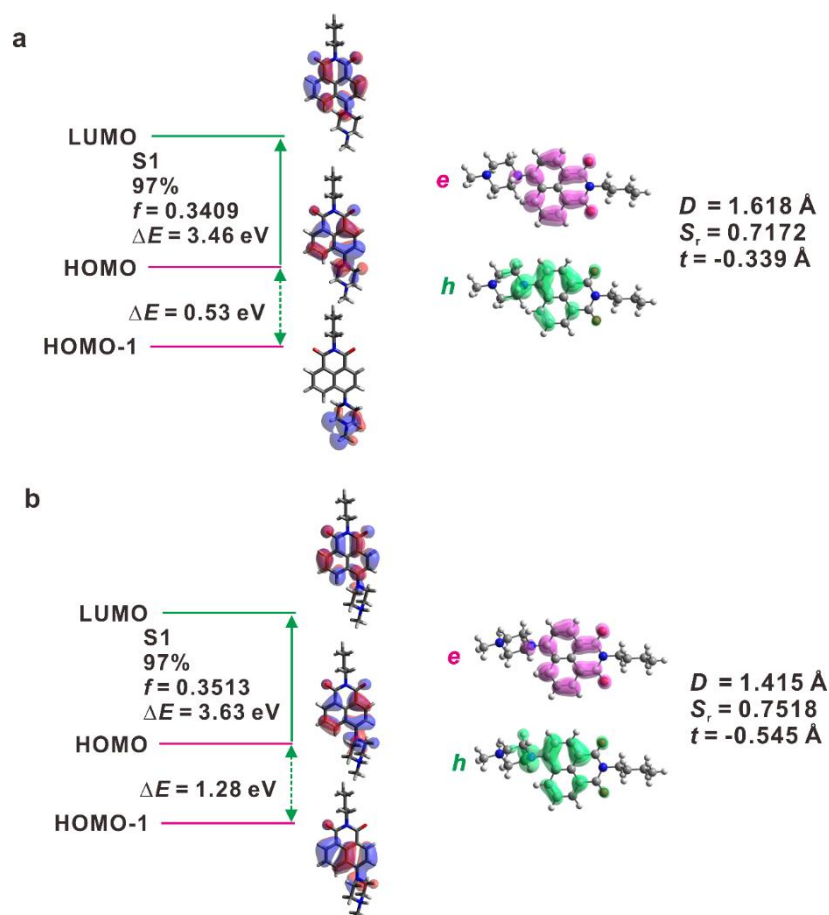


Figure S4. Distribution of molecular frontier orbitals, electronic transitions, and hole-electron analysis (a) before the protonation of **M3** and (b) after the protonation of **M3**. Green donates hole and pink for electron;  $D$  is the centroid distance of hole and electron;  $S_r$  is overlap between hole and electron;  $t$  index

is designed to measure the degree of hole and electron separation in the charge transfer direction.

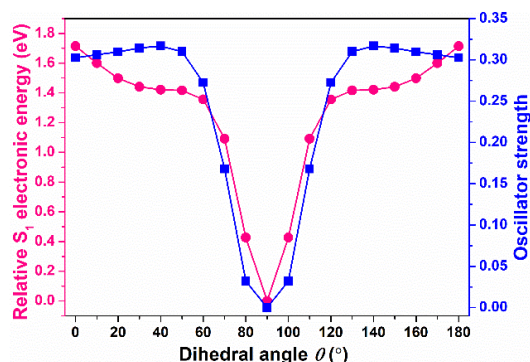


Figure S5. Potential energy surface (pink) of **M3** in the  $S_1$  state and corresponding oscillator strength (blue) in acetonitrile, calculated using M062X.

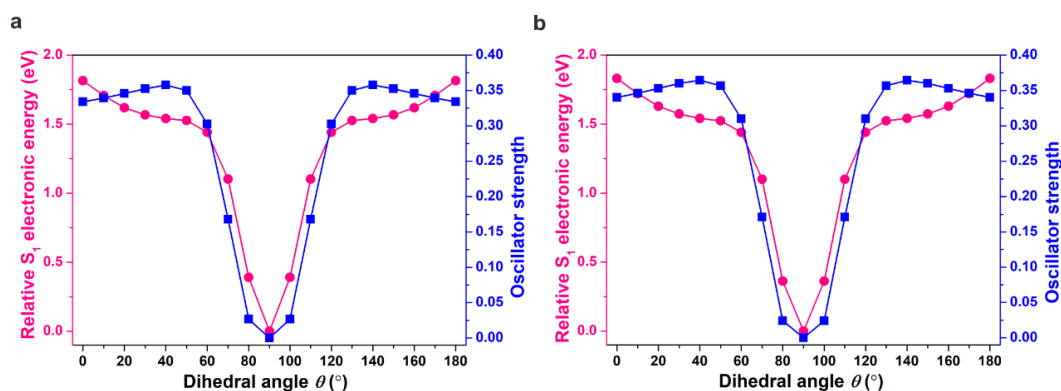


Figure S6. Potential energy surface (pink) and corresponding oscillator strength (blue) of **M1** in the  $S_1$  state in acetonitrile, calculated using CAM-B3LYP (a) and  $\omega$ B97XD (b) functionals.

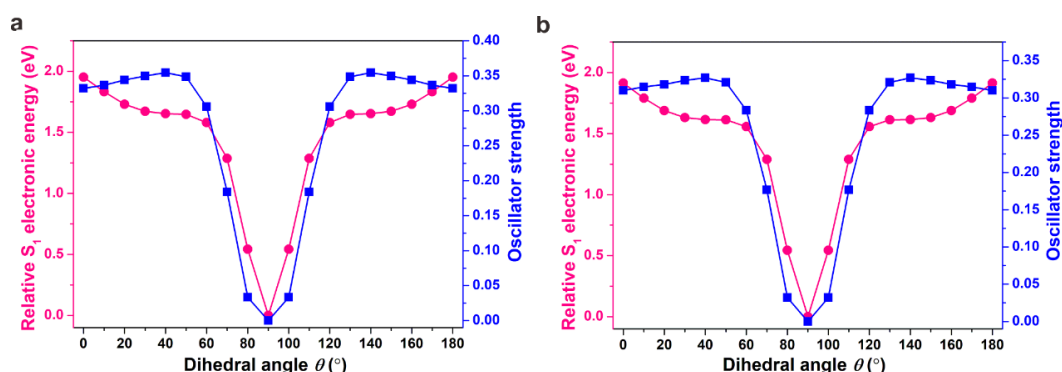


Figure S7. Potential energy surface (pink) and corresponding oscillator strength (blue) of **M1** (a) and **M3** (b) in the  $S_1$  state in water, calculated using M062X functional.

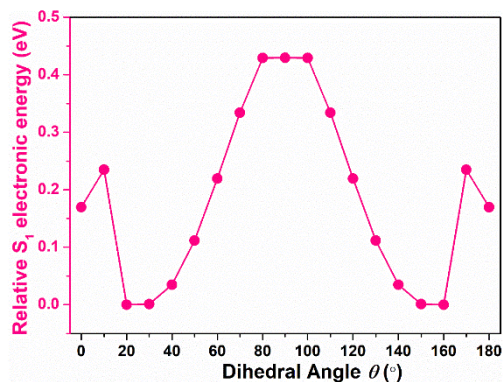


Figure S8. Relative potential energy surface (pink) of **M1-1H** in the  $S_1$  state in acetonitrile, calculated using M062X in combination with liner solvation model.

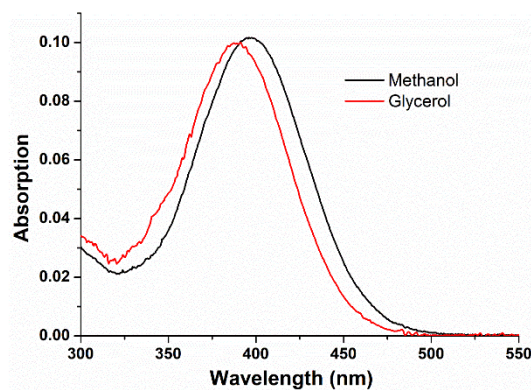


Figure S9. UV-vis absorption spectra of **M3** in methanol and glycerol ( $[M3] = 10 \mu M$ ).

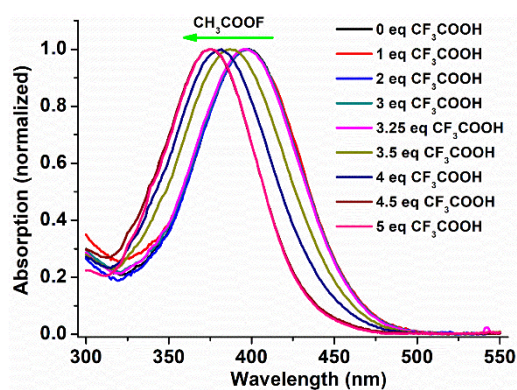


Figure S10. Normalized UV-vis absorption spectra of **M3** upon titration with 0 – 5 eq. of  $CF_3COOH$  in methanol.

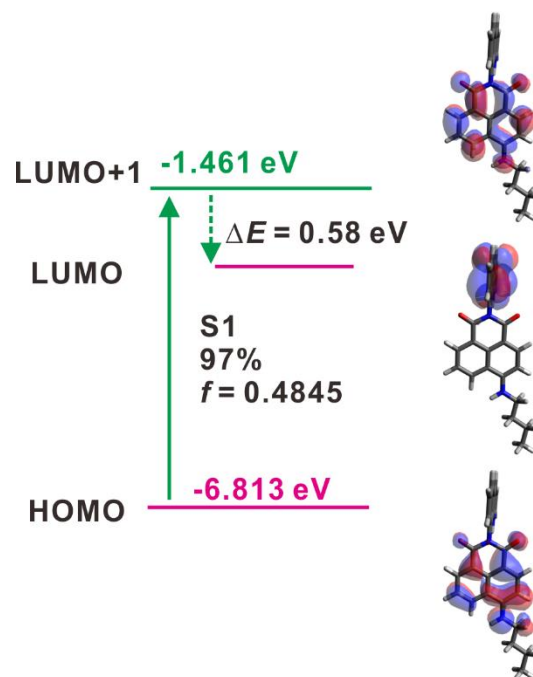


Figure S11. Molecular frontier orbitals and electronic transitions of **M2** in acetonitrile.

#### Reference

1. T. Le Bahers, C. Adamo and I. Ciofini, *J. Chem. Theory Comput.*, 2011, **7**, 2498-2506.